JMEPEG (2016) 25:3366–3374
DOI: 10.1007/s11665-016-2075-7 ©The Author(s). This article is published with open access at Springerlink.com 1059-9495/$19.00

CrossMark

Interfacial Reactions of Zn-Al Alloys with Na Addition on Cu Substrate During Spreading Test and After Aging Treatments

Tomasz Gancarz, Janusz Pstruś, and Katarzyna Berent

(Submitted October 28, 2015; in revised form April 12, 2016; published online April 26, 2016)

Spreading tests for Cu substrate with Zn-Al eutectic-based alloys with 0.2, 0.5, and 1.0 wt.% of Na were studied using the sessile drop method in the presence of QJ201 flux. Spreading tests were performed for 1, 3, 8, 15, 30, and 60 min of contact, at the temperatures of 475, 500, 525, and 550 °C. After cleaning the flux residue from solidified samples, the spreading area of Zn-Al + Na on Cu was determined in accordance with ISO 9455-10:2013-03. Selected, solidified solder-substrate couples were cross-sectioned and subjected to scanning electron microscopy of the interfacial microstructure. The experiment was designed to demonstrate the effect of Na addition on the kinetics of formation and growth of CuZn, Cu_5Zn_8, and $CuZn_4$ phases, which were identified using x-ray diffraction and energy-dispersive spectroscopy analysis. The addition of Na to eutectic Zn-Al caused the spreading area to decrease and the thickness of intermetallic compound layers at the interface to reduce. Samples after the spreading test at 500 °C for 1 min were subjected to aging for 1, 10, and 30 days at 120,170, and 250 °C. The greater thicknesses of IMC layers were obtained for a temperature of 250 °C. With increasing Na content in Zn-Al + Na alloys, the thickness reduced, which correlates to the highest value of activation energy for Zn-Al with 1% Na.

Keywords aging, IMCs, lead-free solder, spreading test, Zn-Al-Na

1. Introduction

The addition of Na to eutectic Zn-Al produces the $NaZn_{13}$ precipitates that caused increased mechanical properties of cast alloys (Ref 1). The alloying additions have a significant impact on properties of cast alloys and on the soldering process, as shown in previous studies for Ag (Ref 2), Cu (Ref 3, 4), In (Ref 5), and Sn (Ref 6). The addition of alloying elements to Zn-Al should block the growth of intermetallic compounds (IMCs) at the interface of liquid solder and in the Cu substrate. The optimal thickness of IMCs, in the CuZn, Cu_5Zn_8, and $CuZn_4$ phases, reduce diffusion of Cu to the solder. The Zn bonded with Na formed $NaZn_{13}$ precipitates which could reduce the thickness of IMC layer at the interface. A similar effect was observed with the addition of Ag content to Zn-Al, which confirms the assumption that precipitates of $AgZn_3$ are produced with Zn and reduce the thickness of IMC layer at the interface (Ref 2). In case of Cu additions to Zn-Al, the Cu and Zn formed CuZn, Cu_5Zn_8, and $CuZn_4$ IMCs, although this had no impact on the growth of IMC layers at the interface (Ref 3, 4). Even, Kang et al. (Ref 7) observed that increasing Al and Cu concentrations in solder caused the spreading area to reduce. As expected, the increasing wettability and IMC layer growth at the interface, caused by alloying elements (Ref 2-7), improved the mechanical properties of the joint. The possibility of using Zn-Al alloys to Al/Cu (Ref 8), Al/Mg (Ref 9), Al/steel (Ref 10), and Cu/Cu (Ref 11) joints, as solders, extends the potential applications in industry. However, there have been few studies on the influence of time, temperature, and alloying elements in the soldering process on spreadability and the growth of the IMC layer at the interface. The study of Zn-Al with Ag content (Ref 2) and Zn-Al with Cu content (Ref 4, 12), on Cu substrate, confirms that a small addition of Ag or Cu reduces the thickness of IMC layers at the interface. Increasing time and temperature caused increasing diffusion of Cu to solder and the growth of IMC layers, most notably regarding the growth of the Cu_5Zn_8 layer, which is characterized by the lowest Gibbs free energy (Ref 2). Moreover, the Al_4Cu_9 phase formed at the interface inside the Cu_5Zn_8 layer which is in accordance with the phase diagram of the Al-Cu-Zn system (Ref 13).

The aim of this study is to demonstrate the effect of Na addition on the kinetics of the formation and growth of the CuZn, Cu_5Zn_8, and $CuZn_4$ phases, during the spreading test and after aging treatments.

2. Experimental

The Zn-Al cast alloys with 0.2, 0.5, and 1.0 wt.% of Na (Ref 1) were studied using the sessile drop method in the presence of QJ201 flux. The experiments without flux were unsuccessful,

This article is an invited submission to JMEP selected from presentations at the Symposium "Wetting and High-Temperature Capillarity," belonging to the Topic "Joining and Interfaces" at the European Congress and Exhibition on Advanced Materials and Processes (EUROMAT 2015), held September 20-24, 2015, in Warsaw, Poland, and has been expanded from the original presentation.

Tomasz Gancarz and **Janusz Pstruś**, Institute of Metallurgy and Materials Science, Polish Academy of Sciences, 30-059 Kraków, Poland; and **Katarzyna Berent**, AGH University of Science and Technology, Academic Centre for Materials and Nanotechnology, 30-059 Kraków, Poland. Contact e-mail: tomasz.gancarz@imim.pl.

as the surface of the solder was oxidized, resulting in a failure to connect with Cu substrate. Therefore, flux QJ201 from powder, consisting of KCl 50 wt.%, LiCl 32 wt.%, NaF 10 wt.%, and $ZnCl_2$ 8 wt.%, was applied for the purposes of protection and oxide removal. Wetting tests were performed after 1, 3, 8, 15, 30, and 60 min of contact, at the temperatures of 475, 500, 525, and 550 °C. As described in Ref 2, the spreading area of 0.5 g samples of Zn-Al-Na solder was calculated after cleaning the flux residue from solidified samples. The spreading area of Zn-Al + Na alloys on Cu substrate was determined in accordance with ISO 9455-10:2013-03. Selected solder/substrate couples were cut perpendicular to the plane of the interface using a diamond wire saw, then mounted in conductive resin, ground, polished, and subjected to microstructure and elemental analyses using scanning electron microscopy (SEM) coupled with energy-dispersive spectrometry (EDS) and x-ray diffraction (XRD) analysis to study the interfacial microstructure and IMCs occurring at the interface. For all samples, three measurements were made at different areas to improve counting statistics and to check the homogeneity of the joints. The XRD measurement was performed in the center of the joint and on the opposite edges. The stress investigation was carried out with the basic assumptions known from the traditional $\sin_2\psi$ method, with the use of the D8 Discover Bruker diffractometer equipped with a parallel-beam primary optics PolyCap system completed a pinhole collimator (1.0 mm aperture) for Cu Kα radiation (λ = 1.7903 Å) and a linear position-sensitive detector LynxEye (range 2.6° on 2θ), capable of working in a parallel secondary beam configuration with the use of Soller collimators. The accelerating voltage and the applied current were 40 kV and 35 mA, respectively. The thickness of the IMC layer (d) is dependent on the growth rate (k) and growth time (t) versus exponential factor (n):

$$d = k(t)^n. \quad \text{(Eq 1)}$$

The growth rate for interface migration is described by an Arrhenius-type equation as follows:

$$k = k_0 \exp\left(-\frac{Q}{RT}\right), \quad \text{(Eq 2)}$$

where k_0, Q, R, and T represent the migration rate constant, the activation energy, the universal gas constant, and the absolute temperature, respectively. Cross-sections after spreading test at 500 °C for 1 min were subjected to aging for 1, 10, and 30 days at 120, 170, and 250 °C. The growth rate and activation energy of the Cu_5Zn_8 layer in the solid state were determined.

3. Results and Discussion

3.1 Reaction of Solders with Substrate Interactions

The characteristics of cast Zn-Al + Na alloys (Ref 1) undergoing the soldering process on a Cu substrate were determined in relation to time and temperature dependencies. The spreading areas of Zn-Al + Na alloys for spreading test at 500 °C after 1, 3, 8, 15, 30, and 60 min of contact and at the temperatures of 475, 500, 525, and 550 °C after 8 min are shown in Fig. 1(a) and (b), respectively. Compared to eutectic Zn-Al, an increased spreading area was observed for Zn-Al alloys with Na content. The increased Na content in Zn-Al alloys did not cause the spreading area to increase for similar time and temperature dependencies. However, the spreading area increased as time (Fig. 1a) and temperature (Fig. 1b) increase. For Zn-Al + Na alloys, the effect was greater for longer times (30 and 60 min) and higher temperatures (525 and 550 °C), compared to eutectic Zn-Al. Although the addition of Ag to Zn-Al alloys caused the formation of $AgZn_3$ IMCs, as Na content $NaZn_{13}$, the spreading area of the Zn-Al + Ag alloys was lower compared to eutectic Zn-Al (Ref 2). The spreading area of the Zn-Al + Cu alloys (Ref 4) was similar to or lower than that of eutectic Zn-Al, although IMCs of Cu_5Zn_8 and $CuZn_4$ were formed inside the solder and at the interface during spreading tests. Additions of Ag, Cu, and Na to Zn-Al alloys caused the formation of IMCs, but in the spreadability tests the most important were the surface active elements, which shows Na. Flux could have a decisive impact on the spreading area. Flux QJ201 was used for Zn-Al + Na, and flux Alu33 for Zn-Al + Ag and Zn-Al + Cu.

The microstructures of Zn-Al with 1.0% Na alloys on Cu substrates after the spreading test at a temperature of 500 °C for the times of (a) 1, (b) 3, (c) 8, (d) 15, (e) 30, and (f) 60 min are presented in Fig. 2. At the interface, the three IMCs (CuZn,

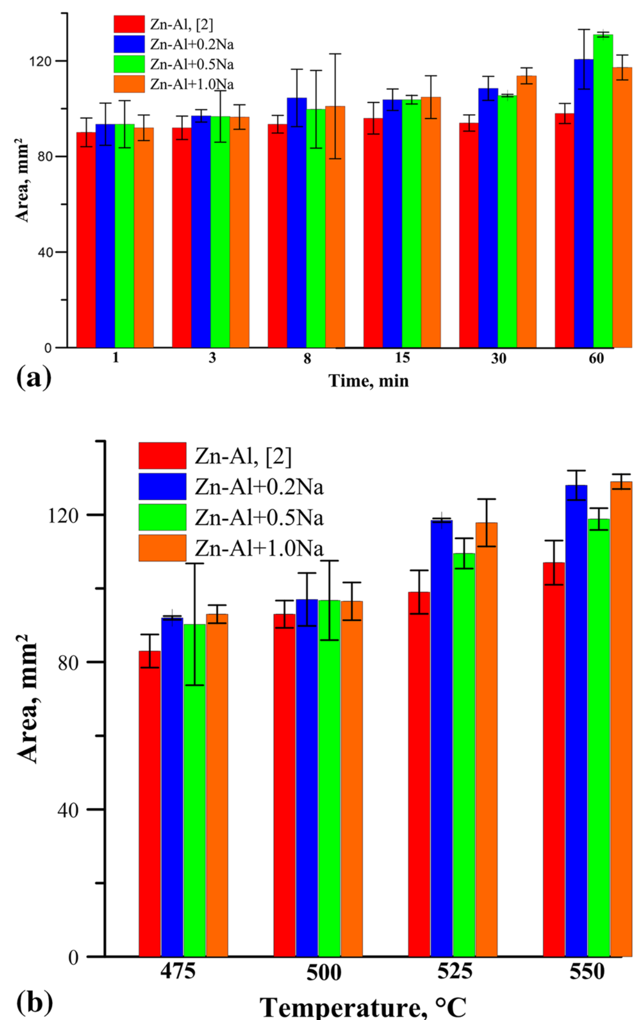

Fig. 1 Spreading area of Zn-Al alloys with Na additions: (a) time and (b) temperature dependencies

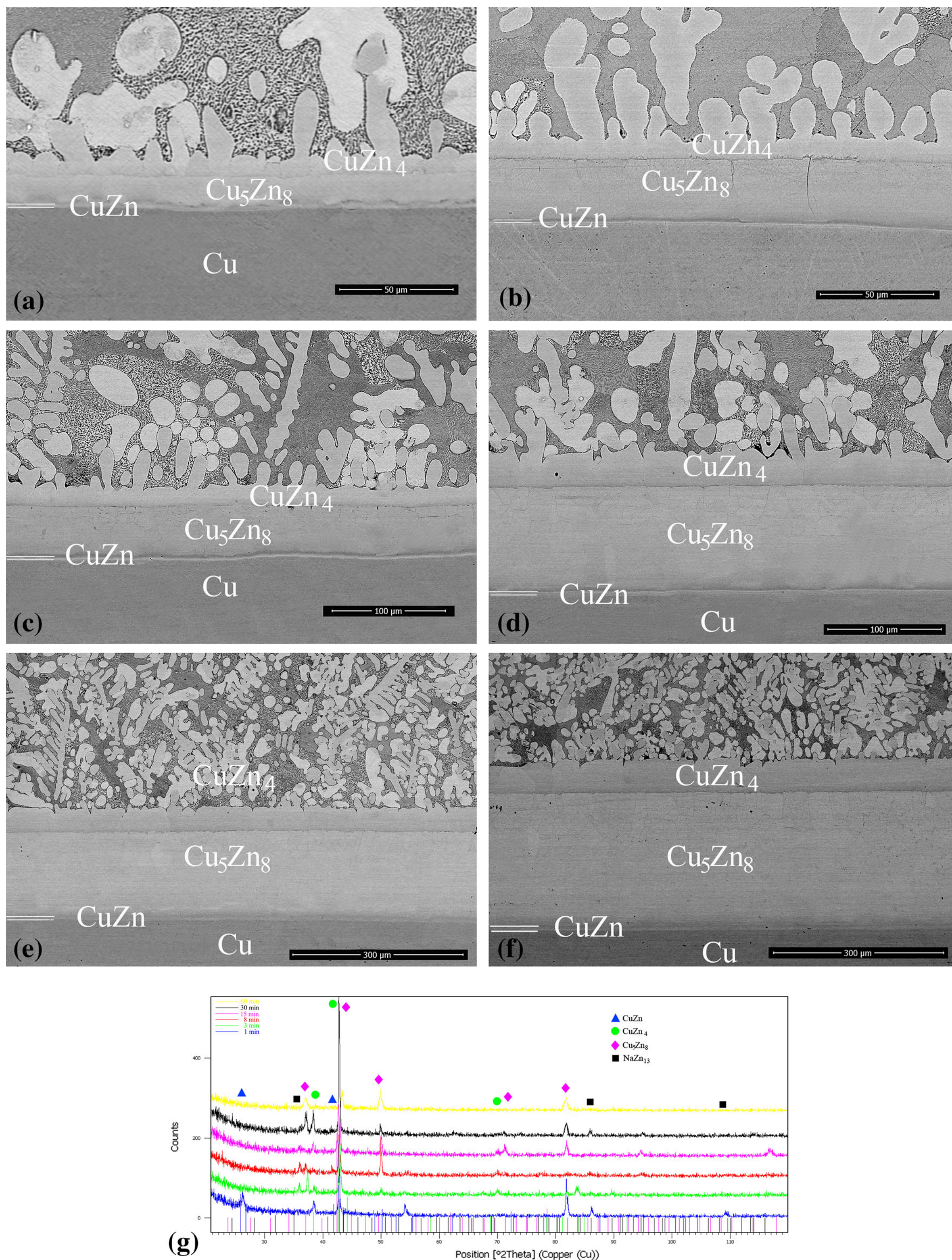

Fig. 2 Microstructures of interfaces on the cross-sections of Zn-Al with 1.0% Na alloys on Cu substrates after spreading test at a temperature of 500 °C for a time of (a) 1 min, (b) 3 min, (c) 8 min, (d) 15 min, (e) 30 min, and (f) 60 min, and (g) XRD analysis results (starting from 60 min on the top to 1 min at the figure's bottom)

Cu_5Zn_8, and $CuZn_4$) were observed from the Cu substrate side, for all times. The formation of IMCs was confirmed by XRD analysis (Fig. 2g). With increasing time, the IMCs grew, with the highest growth for the Cu_5Zn_8 phase, which was observed on the microstructure and in the peaks in XRDs. The CuZn phase was a thin layer on the Cu substrate as observed in Ref 2, 4, 8 and confirmed by Liu et al. (Ref 14). Next, the Cu_5Zn_8 phase, of greater thickness than the top layer, shows the fast path of Cu diffusion, which is also observed in Zn-Al with Ag and Cu alloys (Ref 2, 4, 7). The last layer is the $CuZn_4$ phase, at the top of which scallops were formed which detached and moved to the solder. Microstructure and character of changes,

similar to those obtained for Zn-Al + Na alloys, were observed for Ag (Ref 2) and Cu (Ref 4, 7) additions to Zn-Al alloys. From the data of XRD analysis (Fig. 2g), for 1 min the CuZn, $CuZn_4$, and Cu_5Zn_8 phases are observed, and with increasing time the participation is changed. For 60 min, the peaks of Cu_5Zn_8 phase are increased, which is in line with microstructural observation and literature.

In Fig. 3, the dependencies of IMC thickness over time for (a) 0.2 wt.%, (b) 0.5 wt.%, and (c) 1.0 wt.% Na addition to Zn-Al alloy are presented. The thickness of IMCs for all Zn-Al + Na alloys looks similar, with the effect of adding Na to eutectic Zn-Al being a slightly reduced thickness of the IMC layers compared to eutectic Zn-Al (Ref 2). The Cu_5Zn_8 showed the highest growth, followed by $CuZn_4$ and then CuZn. The character and rate of growth are correlated to parameter "*n*" as a coefficient of growth, where $n \ll 0.5$ represents the grain boundary, $n = 0.5$ represents the volume diffusion, and $n = 1$ represents the chemical reaction. The parameter "*n*" is determined from (1). According to *n* calculated for the CuZn, Cu_5Zn_8, and $CuZn_4$ phases, i.e., $n_{Cu_5Zn_8} > n_{CuZn_4} > n_{CuZn}$, which corresponds to the character of growth, the Cu_5Zn_8 phase grows by mixed volume diffusion and chemical reaction, and the CuZn and $CuZn_4$ phases by volume diffusion only. For the Zn-Al alloy with Na content, the coefficients *n* and *k* for the γ-Cu_5Zn_8 phase were of the same level (0.75 and 0.5 for each alloy, respectively), which means that increased Na content in the alloys has no influence on how the γ phase is created. There was a similar effect for β-CuZn, for which *n* and *k* were on the same level (around 0.44 and 0.22 for each of the alloys, respectively). For the ε-$CuZn_4$ phase, the coefficient *n* was around 0.5, but *k* was reducing with increased Na content in the alloys (1.75, 1.10, and 0.91 for 0.2, 0.5, and 1.0 wt.% Na, respectively). The growth of the β and ε phases was controlled by volume diffusion. The obtained values of *k* and *n* for Zn-Al + Na alloys were similar for the β and ε phases, as reported for Zn-Al + Ag (Ref 2) and Zn-Al + Cu (Ref 12). In the case of Zn-Al + Ag (Ref 2) and Zn-Al + Cu (Ref 12), the coefficient *n* was definite at 0.5 for all phases, and growth was controlled by volume diffusion. However, for the γ phase the coefficient *n* was slightly higher (0.87 for Zn-Al + Ag (Ref 15)), but *k* was much lower (around 0.2). Growth was controlled by mixed volume diffusion and chemical reaction, as for Zn-Al + Ag + -Cu, but the thickness of the IMC layers was slightly lower (Ref 15). However, in Ref 15 the soldering process was conducted for joints Cu/solder/Cu, which could have impacted the values of *k* and *n*. Therefore, the growth of IMCs for Zn-Al + Ag and Zn-Al + Cu in Ref 15 was different compared to Zn-Al + Ag (Ref 2) and Zn-Al + Cu (Ref 12). In the present study, it was observed that, in the beginning, the spreading test shows that the Cu substrate dissolved quickly by the liquid solder, followed by the formation of an IMC layer at the interface, so temperature should have a decisive impact on the amount of Cu substrate dissolved. The microstructures of Zn-Al with 0.5% Na on a Cu substrate after soldering for 8 min at the temperatures of (a) 475 °C, (b) 500 °C, (c) 525 °C, and (d) 550 °C are presented in Fig. 4. The formation of IMCs at the interface was confirmed by XRD analysis (Fig. 4e). For the 475 and 500 °C, the peaks for CuZn and $CuZn_4$ are observed in XRDs, moving to higher temperature 525 and 550 °C, the participation for $CuZn_4$ and Cu_5Zn_8 phases increased. With the increasing temperature, the β, ε, and γ phase layers grow, with the γ phase having the greatest thickness. The highest growth of the γ phase with time and temperature is correlated to the stability of phases from the Cu-Zn system (Fig. 5). According to calculations using ThermoCalc, the γ phase that is Cu_5Zn_8 and Al_4Cu_9 (in the phase diagram of Al-Cu-Zn (Ref 13)) has the lowest Gibbs free energy (Fig. 5). At the top of the γ phase

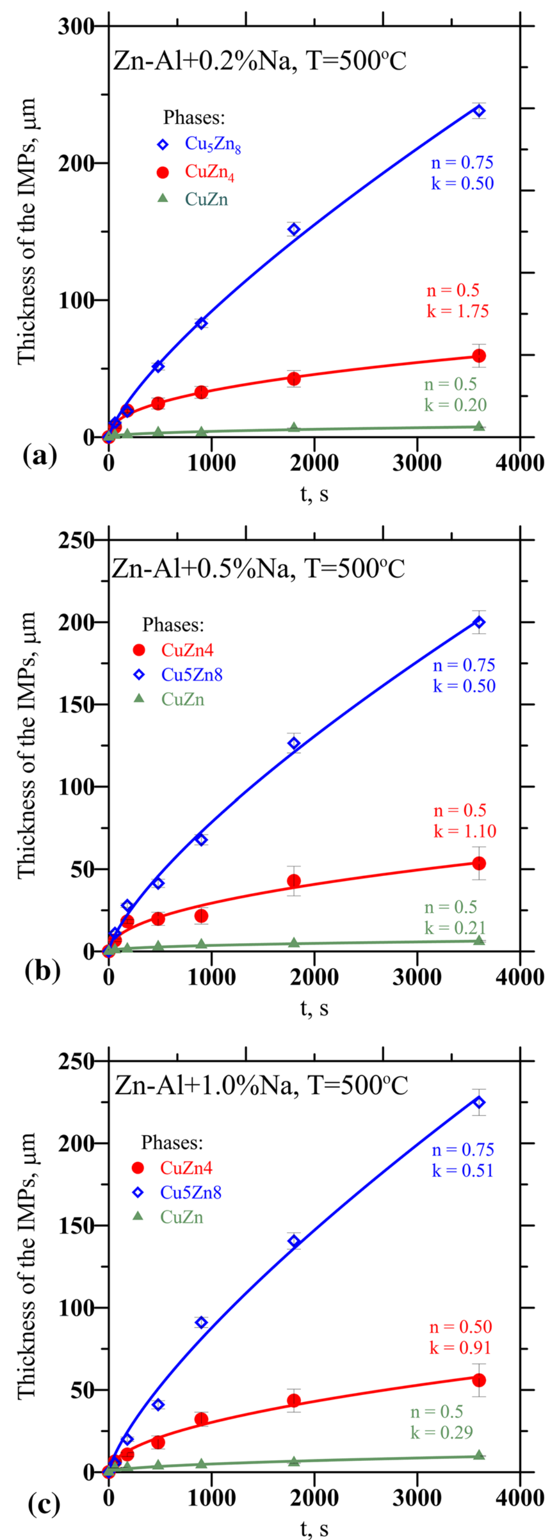

Fig. 3 Dependencies of IMC layer thickness with time for (a) 0.2 wt.%, (b) 0.5 wt.%, and (c) 1.0 wt.% Na addition to Zn-Al alloy

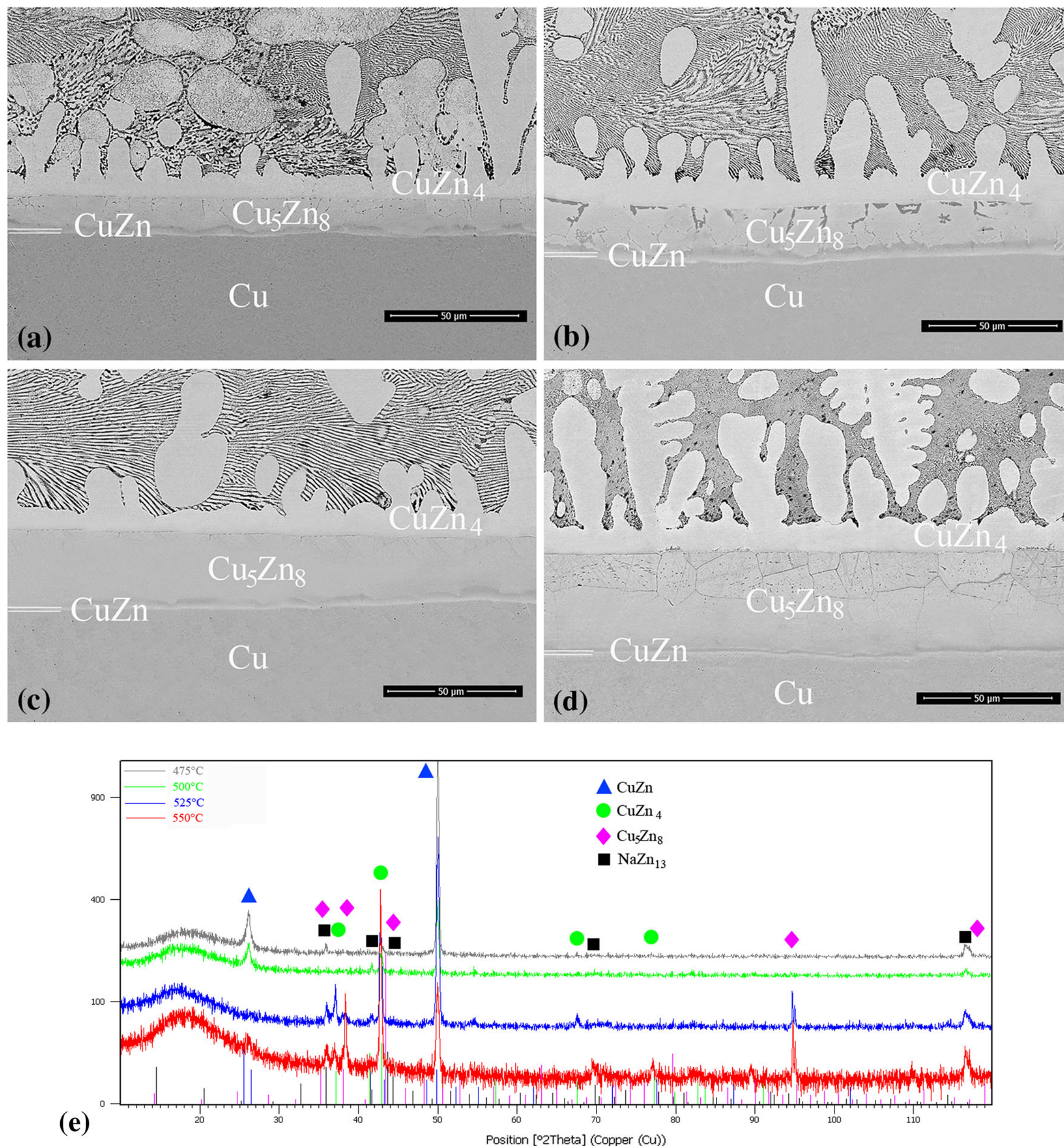

Fig. 4 Microstructure of interfaces on the cross-sections of Zn-Al with 0.5% Na on a Cu substrate after spreading test for 8 min at the temperatures of (a) 475, (b) 500, (c) 525, and (d) 550 °C, and (e) XRD analysis results (starting from 475 on the top to 550 °C at the figure's bottom)

layers, due to the path of the fast diffusing Cu to solder, there appears to be what looks like microcracking in the microstructure (Fig. 4), and start in the formed Al_4Cu_9 phase, which was also confirmed by XRD analysis. The calculated activation energy for Zn-Al + Na alloys on Cu substrate is presented in Table 1. The highest value of activation energy of the γ phases was obtained for Zn-Al + 1.0Na alloy (89.62 kJ/mol) which is two times higher than those for eutectic Zn-Al (Ref 2) and Zn-Al + Cu alloys (Ref 12), and also much higher than that for Zn-Al + Ag alloys (Ref 2). The activation energy of the ε phase, rising with increasing Na content in the alloys, and for the Zn-Al + 0.5Na alloy, is on the same level (~29 kJ/mol) as for eutectic Zn-Al (Ref 2).

3.2 Aging of Joints

The samples (cross-sections) of Zn-Al with 0.2, 0.5, and 1.0 Na content after soldering at 500 °C for 1 min were aged for 1, 10, and 30 days at the temperatures of 120, 170, and 250 °C. The samples were chosen after soldering for 1 min, to show the effect of aging time and temperature for changes to IMCs occurring at the interface. The obtained microstructures after aging were similar for all Zn-Al + Na alloys, with only the thickness of layers at the interface differing with changes to Na content. The microstructures of Zn-Al + 1.0Na, after aging at 120 °C for 1, 10, and 30 days, are presented in Fig. 6. The two layers are observed at the interface, ε ($CuZn_4$) and γ (Cu_5Zn_8 and Al_4Cu_9), which grow as time increases. In the γ layer, fast

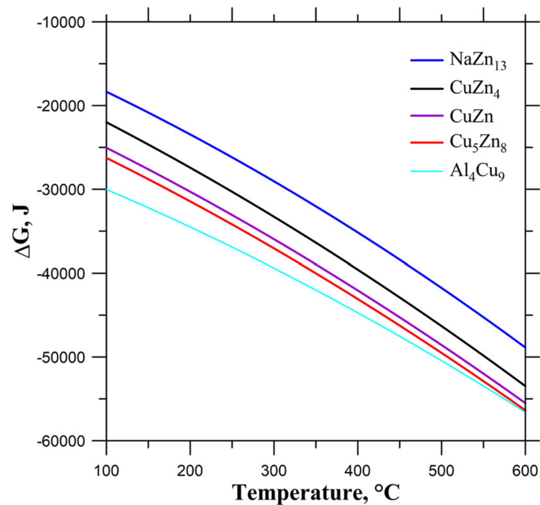

Fig. 5 Temperature dependencies of Gibbs free energy of IMCs, calculated by ThermoCalc

Table 1 Activation energy of IMCs of Zn-Al alloys with Na content after soldering

Alloys	IMCs	Activation energy, *Q*, kJ/mol
Zn-Al (Ref 2)	CuZn	32.38
	Cu_5Zn_8	42.38
	$CuZn_4$	29.54
Zn-Al + 0.2Na	CuZn	59.71
	Cu_5Zn_8	58.10
	$CuZn_4$	13.15
Zn-Al + 0.5Na	CuZn	19.72
	Cu_5Zn_8	80.94
	$CuZn_4$	29.22
Zn-Al + 1.0Na	CuZn	34.08
	Cu_5Zn_8	89.62
	$CuZn_4$	56.02

diffusion of the Cu path formed during soldering created particles of Al_4Cu_9 and grew, as confirmed by EDS analysis (Table 2). The diffusion rate of the Al element in the Cu substrate is slightly higher than that of the Zn element in the Cu substrate (Ref 16). The calculated diffusion rates of Al and Zn elements in the Cu substrate at 450 °C are 5.3×10^{14} and 3.9×10^{14} cm^2/s, respectively (Ref 16). According to Fig. 5, the Gibbs free energy of the Al_4Cu_9 phase is lower than that for the Cu_5Zn_8 phase, and at lower temperatures this difference becomes more marked. However, for aging at 170 °C (Fig. 7), after 1 day (Fig. 7a), a microstructure similar to that after 120 °C was observed in the ε and γ layers, with increasing particles of Al_4Cu_9 in the γ phase. But after 10 days (Fig. 7b) the microstructure changed, the ε phase was consumed by the γ phase, and particles of Al_4Cu_9 phase dissolved in Cu_5Zn_8. This effect is associated with increasing the temperature to 170 °C, which caused increasing diffusion of Cu to the solder and a greater amount of free Zn, which created a Cu_5Zn_8 layer with Al dissolving inside. A similar effect was observed by Wang (Ref 17) for SnZn on Cu, for aging at 170 °C, though the highest stability of the Cu_5Zn_8 layer with increased time caused the creation of a Cu_6Sn_5 phase. This was caused by the diffusion of Cu to the solder and the availability of Sn at the

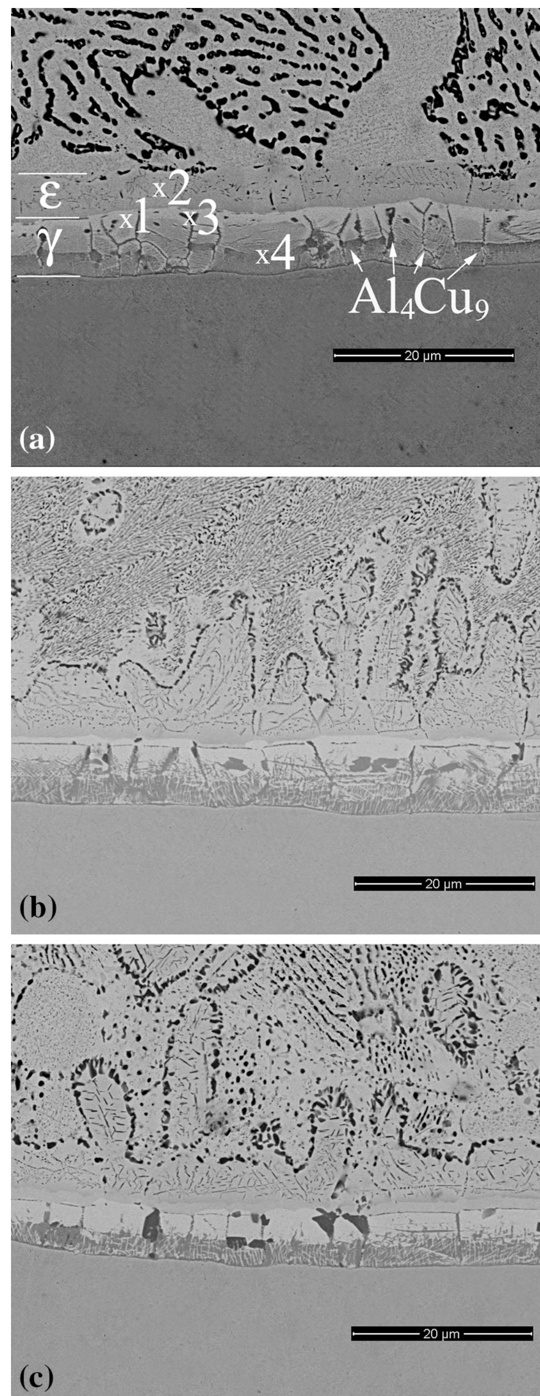

Fig. 6 Microstructure of Zn-Al + 1.0Na after aging process at a temperature of 120 °C for (a) 1, (b) 10, and (c) 30 days

interface. After 30 days (Fig. 7c), the thickness of the Cu_5Zn_8 layer grew, and the microstructure was almost the same as that after 10 days. On increasing the aging temperature to 250 °C, the γ-Cu_5Zn_8 layer grew much faster, resulting in a γ layer several times thicker than that obtained by aging at 170 °C for the same time. The microstructures of Zn-Al + 1.0Na, after aging at 250 °C, are presented in Fig. 8(a), (b), and (c) for 1, 10, and 30 days, respectively. At the interface, in the γ-Cu_5Zn_8 layer, and at the top, close to the solder drop, particles of the

Table 2 EDS analysis of Zn-Al + 1.0Na at the points marked in Fig. 6 and 7

Marked point	Al, at.%	Cu, at.%	Zn, at.%
1	9.8	41.7	48.6
2	0.7	17.6	81.7
3	22.2	46.9	30.9
4	11.7	45.2	43.1
5	55.3	34.3	10.4
6	9.5	40.5	50.0
7	34.0	41.4	24.6
8	3.2	34.5	62.3

Al_4Cu_9 phase are observed. In the EDS analysis, the Na was not taken into consideration, because the Zn^L and Na^K appear close to each other, and therefore the EDS analysis of Na was not reported in Table 2. The initial thickness of each IMC layer after the aging process should be taken into account, and in Eq 1 should be modified as

$$\Delta x = d_0 + kt^n, \qquad \text{(Eq 3)}$$

where Δx is the average thickness of the IMC layer, d_0 is the initial thickness of the IMC layer, k is the growth rate coefficient, and t is the aging duration.

The dependencies of thickness of the γ layer versus time for Zn-Al + Na alloys are shown in Fig. 9, for the temperatures of (a) 120, (b) 170, and (c) 250 °C. At higher aging temperature, the γ layer grew faster, but with the addition of increased Na content to Zn-Al alloys the thickness of IMC layer is reduced. This effect was caused by Zn bonded with Na and forming $NaZn_{13}$ precipitates, which block the growth of the γ layer at the interface. The formation of the $NaZn_{13}$ phase was confirmed by XRD analysis. The thickness of the IMC layer for Zn-Al-Na alloys at the interface after aging was less than the values for Zn-4Al obtained by Takaku et al. (Ref 12). The three β, ε, and γ phases' layers were observed in Ref 12 after annealing, even at temperatures as high as 200 and 300 °C. For the Zn-Al + Na alloys on Cu substrate at high temperatures, only the γ phase was observed and grew. The obtained growth rates for the Zn-Al + Na γ phase (Table 3), compared with Zn-Al and Zn-Al + Cu (Ref 12), are orders of magnitude smaller for each temperature. The activation energy for the γ phase was also much higher for the Zn-Al + Na, at 65.69, 66.20, and 73.11 kJ/mol for 0.2, 0.5, and 1.0 wt.% Na content, compared to 44.37 kJ/mol for Zn-4Al (Ref 12) and 39.03 kJ/mol for Zn-4Al1Cu (Ref 12). Taking into account the growth rate and activation energy data obtained from the aging process, it can be said that the amount of Na in Zn-Al alloys influences the number of $NaZn_{13}$ precipitates at the interface, and also has a great impact on phenomena occurring there.

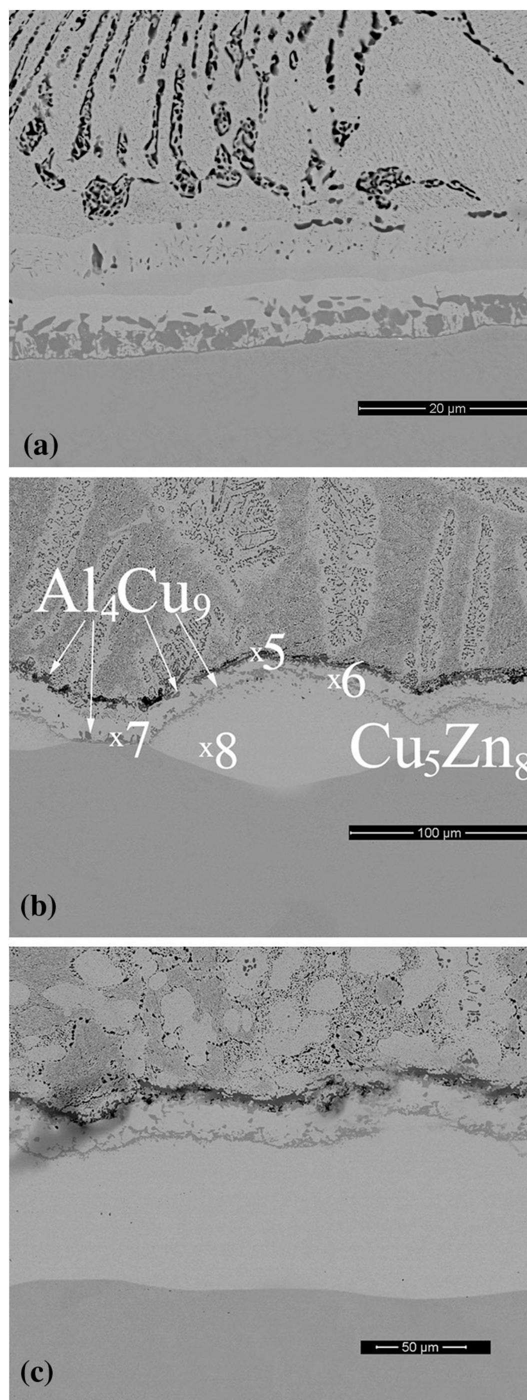

Fig. 7 Microstructure of Zn-Al + 1.0Na after aging process at a temperature of 170 °C for (a) 1, (b) 10, and (c) 30 days

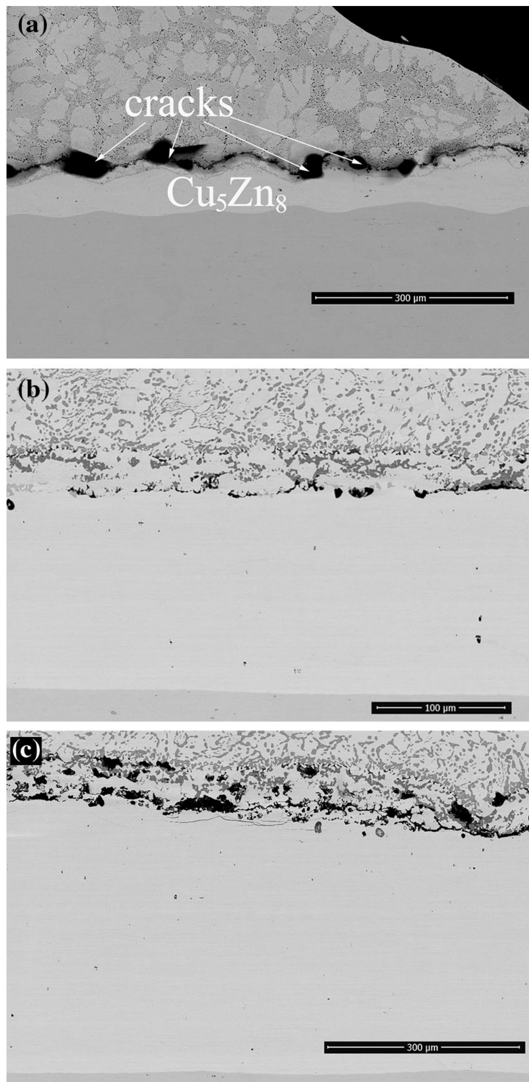

Fig. 8 Microstructure of Zn-Al + 1.0Na after aging process at a temperature of 250 °C for (a) 1, (b) 10, and (c) 30 days

4. Conclusions

The effects of spreading time and temperature on the creation of IMC layers of lead-free Zn-Al-xNa solder alloys on Cu substrates were investigated. The addition of 0.2% Na to Zn-Al caused the spreading area to expand, while the addition of greater amounts of Na did not cause any further expansion of the spreading area. Increasing Na content in Zn-Al alloys caused the growth rate of the Cu_5Zn_8 phase to remain constant, the $CuZn_4$ phase to decrease, and the CuZn phase to increase, over time, at 500 °C. The growth of IMCs during soldering on the Cu substrate was found to be controlled by volume diffusion for CuZn and $CuZn_4$ phases, but by mixed volume diffusion and chemical reaction for the Cu_5Zn_8 phase. Higher activation energies were observed compared to eutectic Zn-Al, and the activation energy increased with increasing Na content in Zn-Al alloys. In the spreading test, the thickness of IMC layers for all ZnAl + Na alloys increased with increased time and temperature. The higher growth of the γ layer was observed, as was the fast diffusion path of Cu that started to create the Al_4Cu_9 phase,

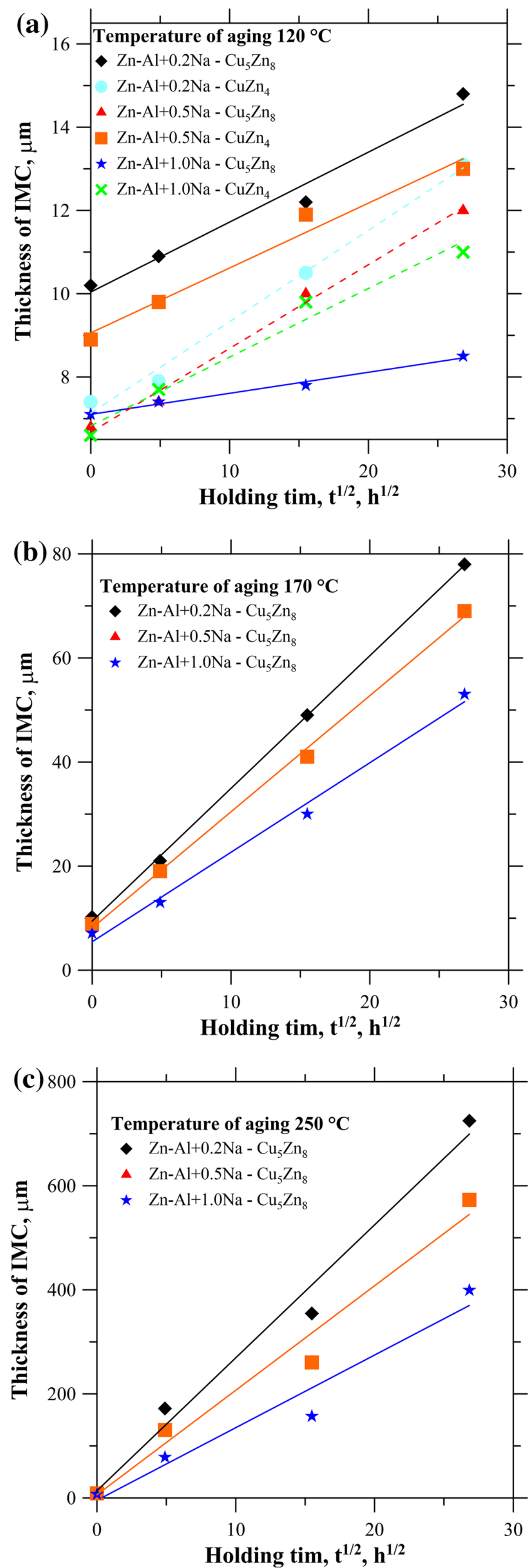

Fig. 9 Dependencies of IMC layer thickness vs. time for Zn-Al + Na alloys after aging process at the temperatures of (a) 120, (b) 170, and (c) 250 °C

which has a lower Gibbs free energy phase (Ref 2). During the aging process, the growth of IMC layers was controlled by volume diffusion. At 120 °C, the ε and γ layers were observed,

Table 3 Properties of IMC growth during aging in Cu/Solid Zn-Al alloys with Na additions

Solder	IMC	*K*, m s$^{1/2}$ 120 °C	170 °C	250 °C	k_0, m s$^{1/2}$	Activation energy, *Q*, kJ/mol)
Zn-Al + 0.2Na	Cu_5Zn_8	1.68E−10	2.55E−09	2.55E−08	1.06E−01	65.69
Zn-Al + 0.5Na		1.56E−10	2.23E−09	2.46E−08	1.13E−01	66.20
Zn-Al + 1.0Na		5.05E−11	1.72E−09	1.40E−08	3.75E−01	73.11

and inside the γ layer there was a particle of the Al_4Cu_9 phase, which increased over time. At higher temperatures (170 and 250 °C in particular), the γ layer thickness grew rapidly, and the small number of particles in the Al_4Cu_9 phase was observed only in the top of the Cu_5Zn_8 layer. Increasing the Na content in the Zn-Al alloy caused an increasing number of $NaZn_{13}$ precipitates, which had a great impact on the creation of IMC layers of lead-free Zn-Al-*x*Na solder alloys.

Acknowledgments

This work was financed by the Minister of Science and High Education of Poland Grant IP2014 011473, in the years 2015-2017.

Open Access

This article is distributed under the terms of the Creative Commons Attribution 4.0 International License (http://creativecommons.org/licenses/by/4.0/), which permits unrestricted use, distribution, and reproduction in any medium, provided you give appropriate credit to the original author(s) and the source, provide a link to the Creative Commons license, and indicate if changes were made.

References

1. T. Gancarz, G. Cempura, and W. Skuza, Characterization of ZnAl Cast Alloys with Na Additions, *Mater. Character.*, 2016, **111**, p 147–153
2. T. Gancarz, J. Pstruś, P. Fima, and S. Mosińska, Effect of Ag Addition to Zn-12Al Alloy on Kinetics of Growth of Intermediate Phases on Cu Substrate, *J. Alloys Compd.*, 2014, **582**, p 313–322
3. X. Yan, S. Liu, W. Long, J. Huang, L. Zhang, and Y. Chen, The Effect of Homogenization Treatment on Microstructure and Properties of ZnAl15 Solder, *Mater. Des.*, 2013, **45**, p 440–445
4. T. Gancarz, J. Pstruś, S. Mosińska, and S. Pawlak, Effect of Cu Addition to Zn-12Al Alloy on Thermal Properties and Wettability on Cu and Al Substrates, *Met. Mater. Trans. A*, 2016, **47**, p 368–377
5. T. Gancarz, J. Pstruś, P. Fima, and S. Mosińska, Thermal Properties and Wetting Behavior of High Temperature Zn-Al-In Solders, *J. Mater. Eng. Perform.*, 2012, **21**, p 599–605
6. X. Yang, W. Hu, X. Yan, and Y. Lei, Microstructure and Solderability of Zn-6Al-xSn Solders, *J. Electron. Mater.*, 2015, **44**, p 1128–1133
7. N. Kang, H. Na, S. Kim, and C. Kang, Alloy design of Zn-Al-Cu Solder for Ultra High Temperatures, *J. Alloys Compd.*, 2009, **467**, p 246–250
8. F. Ji, S. Xue, J. Lou, Y. Lou, and S. Wang, Microstructure and Properties of Cu/Al Joints Brazed with Zn-Al Filler Metals, *Trans. Nonferrous Met. Soc. China*, 2012, **22**, p 281–287
9. L. Ma, D. He, X. Li, and J. Jiang, High-Frequency Induction Soldering of Magnesium Alloy AZ31B Using a Zn-Al Filler Metal, *Mater. Lett.*, 2010, **64**, p 596–598
10. Y. Jinlong, X. Songbai, X. Peng, L. Zhaoping, D. Wei, and Z. Junxiong, Development of Novel CsF-RbF-AlF3 Flux for Brazing Aluminium to Stainless Steel with Zn-Al Filler Metal, *Mater. Des.*, 2014, **64**, p 110–115
11. M. Prach and R. Kolenak, Soldering of Copper with High-Temperature Zn-Based Solders, *Procedia Eng.*, 2015, **100**, p 1370–1375
12. Y. Takaku, L. Felicia, I. Ohnuma, R. Kainuma, and K. Ishida, Interfacial Reaction Between Cu Substrates and Zn-Al Base High-Temperature Pb-Free Solders, *J. Electron. Mater.*, 2008, **37**, p 314–323
13. V. Raghavan, Al-Cu-Zn, *J. Phase Equilib. Diff.*, 2007, **28**, p 183–188
14. X. Liu, B. Doung, D. Zhao, and X. Zhu, Microstructures and Properties of Tungsten Inert Gas Welding Joint of Super-Eutectic ZA Alloy, *Trans. Nonferrous Met. Soc. China*, 2001, **11**, p 387–390
15. J. Pstrus and T. Gancarz, Interfacial Phenomena in Al/Al, Al/Cu, and Cu/Cu Joints Soldered Using an Al-Zn Alloy with Ag or Cu Additions, *J. Mater. Eng. Perform.*, 2014, **23**, p 1614–1624
16. Y. Xiao, M. Li, L. Wang, S. Huang, X. Du, and Z. Liu, Interfacial Reaction Behavior and Mechanical Properties of Ultrasonically Brazed Cu/Zn-Al/Cu Joints, *Mater. Des.*, 2015, **73**, p 42–49
17. J. Wang, C. Lin, and C. Chen, Retarding the Cu5Zn8 Phase Fracture at the Sn-9 wt% Zn/Cu Interface, *Scr. Mater.*, 2011, **64**, p 633–636